A model study on the relation between atmospheric boundary-layer dynamics and poleward atmospheric moisture transport in Antarctica

By N. P. M. VAN LIPZIG[1]* and M. R. VAN DEN BROEKE[2], [1]*Royal Netherlands Meteorological Institute (KNMI), P.O. Box 201, 3730 AE, de Bilt, The Netherlands;* [2]*Institute for Marine and Atmospheric Research Utrecht (IMAU), P.O. Box 80 005, 3508 TA, The Netherlands*

ABSTRACT

A regional atmospheric model was used to study the relationship between atmospheric boundary-layer dynamics and moisture transport toward the Antarctic grounded ice sheet. The model was integrated for a 14-yr period (1980–1993) using a grid spacing of 55 km. Re-analyses from the European centre for medium-range weather forecasts were used to force the model from the lateral boundaries. Sea surface temperature and sea ice extent were prescribed from daily observations. It was found that the boundary layer responds passively to the large-scale circulation rather than being the driving force for the meridional circulation and moisture advection toward the ice sheet. Moisture transport by the mean circulation is directed from the ice sheet toward the Southern Ocean and transient eddies are responsible for the moisture transport toward the ice sheet. Frequent interruption of the katabatic winds by passing low-pressure systems characterise years with a large poleward moisture transport. Therefore there is a negative correlation between the annual mean poleward moisture transport and both the directional constancy and the southerly wind component in the boundary layer near the ice edge. A case study for July 1980 shows that the wind and the specific humidity in the middle and higher troposphere determine the poleward atmospheric moisture transport in Wilkes Land and that the moisture advection in the boundary layer is insignificant in this region.

1. Introduction

Poleward atmospheric moisture transport roughly balances the primary components of the surface mass balance of the Antarctic ice sheet, namely precipitation and sublimation. Surface mass balance processes are widely studied because of their importance for global sea level change, but also because of their effect on signals archived in ice cores (e.g. Krinner et al., 1997; Steig et al., 1994). These ice core signals are an important source of information on past variations in mete-

orological variables such as temperature and chemical tracers (e.g. Dansgaard, 1964; Johnsen et al., 1972; Peel et al., 1996). Therefore, improving our understanding of the processes determining the surface mass balance is relevant. In this paper, we focus on the relation between poleward atmospheric moisture transport and meteorological conditions in the atmospheric boundary layer.

The main characteristics of the Antarctic boundary layer are the strong temperature inversion and the associated katabatic winds. Due to continuous radiative cooling, the potential temperature of the air near the surface is lower than the potential temperature of the overlying layer, and the near-surface air becomes negatively buoyant. In sloping regions, a horizontal pressure gradient forces the negatively buoyant air down the slope, deflected by the Coriolis force. The Antarctic

*Corresponding author.
e-mail: nvl@bas.ac.uk
Presently at: British Antarctic Survey, High Cross, Madingley Road, Cambridge CB3 0ET, UK.

wind regime is therefore strongly influenced by the orography of the ice sheet (Parish and Bromwich, 1991).

The radially diverging katabatic outflow is compensated for by an influx of warmer air in the middle troposphere, while subsidence takes place in the interior of the ice sheet. The induced meridional circulation, caused by katabatic winds, suggests an active mass exchange between Antarctica and subpolar latitudes (Parish et al., 1994). An analytical study on the climatic average outflow at the rim of the continent as a function of diabatic cooling in the interior and entrainment of warm air from above the katabatic layer shows that an amount of air, significant even at global scale, is exported from the Antarctic continent (Dalu et al., 1993).

Numerous studies show an interesting interplay between the katabatic and the large-scale circulations. Due to the interaction of circulation with decaying weather systems, cyclonic vorticity is exported in the upper tropospheric westerlies and consequently a strong and persistent drainage flow is maintained (James, 1989). Without the influence of weather systems, the cyclonic vorticity in upper layers would be much larger and the accompanying large-scale pressure gradient would strongly oppose the downslope flow in the katabatic layer. Parish et al. (1993) and Wendler et al. (1997) showed that the large-scale circulation is important for the strengthening and weakening of the katabatic circulation. The same conclusion was reached by Murphy and Simmonds (1993) and Turner et al. (2001), who analysed strong wind events near Casey station. Katabatic winds, in turn, influence the large-scale tropospheric circulation (Parish and Bromwich, 1991) and generate mesoscale atmospheric circulation in coastal regions (Gallée, 1996; Heinemann, 1997). Parish and Bromwich (1998) even speculate that the katabatic wind pattern is the cause of the climatologically favoured positions of the cyclones around the continent. From these studies it is clear that we cannot study the relation between the atmospheric boundary layer and the atmospheric moisture transport properly without considering large-scale circulation.

Radiosonde data have been used to study atmospheric water-vapour transport, but stations are too sparse to obtain a reliable moisture budget estimate for a large area (East Antarctica) (Connolley and King, 1993). Analysis fields from major meteorological centres are constructed by assimilating all available irregularly distributed meteorological data into an integration with a General Circulation Model (GCM). These fields provide important information on the moisture transport in the Antarctic region (e.g. Bromwich et al., 1995; Budd et al., 1995; Genthon and Krinner, 1998; Turner et al., 1999; Noone et al., 1999; Marshall, 2000; Reijmer and van den Broeke, 2001). Cullather et al. (1997a) and Bromwich et al. (1995) showed that for the Antarctic region, analyses from the European Centre for Medium-range Weather Forecasts (ECMWF) are generally found superior over analyses from the National Centers for Environmental Prediction (NCEP) and from the Australian Bureau of Meteorology (ABM). There has been discussion on whether ECMWF operational analyses or re-analyses (ERA-15) (Gibson et al., 1997) better represent year-to-year variability in moisture transport. Genthon and Krinner (1998) pointed out that variability of the operational analyses can be biased by changes in the meteorological model and assimilation techniques during the period studied, whereas re-analyses produce more homogeneous time series by using the same meteorological model and assimilation techniques during the period of integration. On the other hand, Bromwich et al. (2000) showed that an error in the ERA-15 assimilation of data from the Antarctic station Vostok results in a different flow pattern in ERA-15 compared to the operational analyses, which affects the mean moisture flux in the West Antarctic sector (75°–90°S, 120°–180°W). In addition to this problem, ERA-15 shows a pronounced decoupling of the lowest atmospheric layer from the overlying atmosphere (Connolley and Harangozo, 2001; Van Lipzig et al., 1999).

The horizontal grid spacing in an atmospheric model plays a key role in studies on katabatic winds, since it determines to which extent the orography is resolved. Connolley and Cattle (1994) showed that katabatic winds are realistically represented in a $2.5° \times 3.75°$ latitude–longitude grid (GCM), but that small-scale confluence patterns in individual valleys are not resolved. In addition, a coarse resolution can result in an anomalous model slope, affecting the strength of the katabatic winds (Tzeng et al., 1993). Indeed, Van den Broeke et al. (1997) found that wind speeds are underestimated in coastal regions due to smoothened topography in a $1.1° \times 1.1°$ GCM.

To obtain a higher horizontal resolution $(55 \text{ km})^2$ at reasonable computational cost, we use a regional atmospheric model (RACMO) to study the role of katabatic circulation on moisture transport. Another advantage of RACMO is that it has been modified and

evaluated for Antarctic conditions (Van Lipzig, 1999; Van Lipzig et al., 1998; 1999; Schlosser et al., 2002). Because of the large influence of the synoptic-scale circulation on the katabatic winds, it is important that the model represents the synoptic-scale circulation accurately. This is acieved by forcing RACMO from the lateral boundaries by ERA-15. In the lateral boundary zone of the RACMO domain, extending from 65°S to 47°S, both satellite and in-situ measurements were assimilated into the re-analysis cycle, making the ERA-15 fields less dependent on the model formulation than in the region of the Antarctic ice sheet, where the amount of observations was much smaller. Recently, adjusted versions of RACMO have been used to study meteorological conditions in the Antarctic region (Van den Broeke et al., 2002; Van den Broeke and van Lipzig, 2002; Van Lipzig et al., 2002), the Arctic region (e.g. Dethloff et al., 2001, in this study the model is refered to as HIRHAM) and Europe (e.g. Van Meijgaard et al., 2001; Lenderink and van Meijgaard, 2001; Van den Hurk et al., 2002).

Wind-blown snow is not taken into account in RACMO. Giovinetto et al. (1992) estimated that wind transport of snow across the ice edge is at least one order of magnitude smaller than the atmospheric moisture transport toward the ice sheet. However, preliminary integrations for polar night conditions and without taking into account large-scale circulation suggest that blowing snow may be a significant component for the Antarctic surface mass balance (Gallée et al., 2001), indicating that further insight is needed in snow-erosion processes in Antarctica.

In this paper, we investigate the relationship between poleward atmospheric moisture transport and meteorological conditions in the atmospheric boundary layer. Since katabatic winds strongly interact with large-scale circulation, we also take into account meteorological conditions in the middle and higher troposphere. In Section 2 we give a description of RACMO. In Section 3 we discuss the modelled meridional circulation at the grounding line, defined as the contour line where grounded ice turns into floating ice (ice shelves). The relationship between resolved-scale poleward atmospheric moisture transport and the surface mass balance is described in Section 4. Temporal and spatial variability of the atmospheric moisture transport are discussed in Sections 5 and 6. In Section 7 we focus on Wilkes Land (Fig. 1) to study the episodic nature of atmospheric moisture transport and its relation with local meteorological conditions. Conclusions are given in Section 8.
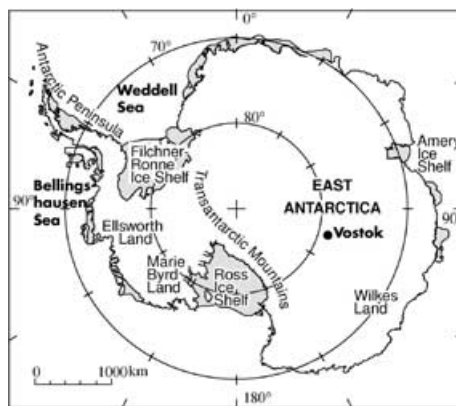
Fig. 1. Regions mentioned in this paper.

2. Model description

Detailed descriptions of RACMO are given by Christensen et al. (1996) and Christensen and van Meijgaard (1992). The dynamical part of RACMO is identical to the High-Resolution Limited Area Model (Gustafsson, 1993). Time integration is done using a leapfrog semi-implicit scheme using a time step of 4 min.

The parameterisations of the physical processes in RACMO are taken from the ECHAM4 GCM (Roeckner et al., 1996). The parameterisation of stratiform clouds uses tendency equations for temperature, specific humidity and specific liquid water (Sundqvist, 1978). The model treats specific liquid water as a prognostic variable, but the distinction into liquid water and ice is diagnosed from temperature. The closure relations are: (i) humidity transport rate is used to moisten a pre-existing cloud, and (ii) the instantaneous evaporation/condensation in the cloud-free part of a grid box is equal to the liquid water transport into this grid box. The cloud cover is diagnosed from the model relative humidity and a prescribed vertical profile of relative humidity acting as a threshold for cloud formation.

The turbulent fluxes at the surface are calculated from Monin–Obukhov similarity theory. Transfer coefficients derived by Louis (1979) are used. A higher-order closure, using a prognostic equation for turbulent kinetic energy, is used to compute turbulent transfer within and above the planetary boundary layer.

The parameterisation of the boundary layer and surface fluxes affect the strength of the katabatic circulation (King et al., 2001), implying that surface heat exchange processes have to be correctly represented

in a model in order to generate a realistic katabatic circulation. Van Lipzig et al. (1999) showed that surface heat exchange processes are adequately represented in RACMO. To achieve this, adjustments were made to the original ECHAM4 model formulation, e.g. taking out the dependency of the surface albedo on the surface temperature, altering the values for the heat capacity and diffusivity of snow, using an improved and more detailed ice sheet orography (British Antarctic Survey et al., 1993) and adding an extra layer in the atmosphere close to the surface to obtain higher resolution in the generally shallow boundary layer of the Antarctic atmosphere. In this configuration, we adopted 20 layers in the vertical with the lowest layers centred at about 7, 35, 130, 330 and 660 m.

The rectangular horizontal grid covers an area of 4.6×10^7 km^2, including the Antarctic continent and part of the Southern Ocean, with a horizontal resolution of about (55 km)^2. ERA-15 fields were used to initialise the prognostic variables. In the lateral boundary zone of the model domain, extending from about 48°S to 62°S, prognostic variables were relaxed toward ERA-15 fields using a technique proposed by Davies (1976). An integration was performed for the 14-year period 1980–1993, for which ERA-15 data were available. Lateral boundaries were updated every 6 h, and the sea surface temperature and sea ice mask were prescribed from daily observations, available from the ERA-15 archive. Note that the sea-ice temperature is a prognostic variable.

The model has been evaluated using in-situ measurements from Antarctica. The spatial pattern of the surface mass balance (B) corresponds closely to compilations of measurements (Van Lipzig et al., 2002), although sublimation is overestimated in mountainous regions. Generally, the RACMO-value for B in the interior of the continent is larger than the values in the operational analyses (Cullather et al., 1997b) and in ERA-15 (Genthon and Krinner, 1998; Turner et al., 1999). Turner et al. (1999) showed that ERA-15 slightly underestimates B in the interior. RACMO is in closer agreement with the measurements in this region. In addition, problems related to overestimation of evaporation/sublimation from the ice shelves, overestimation of the inverstion strength and the westerly displacement of the accumulation on the western side of the Antarctic Peninsula as a result of smoothing of the model orography are found to be much smaller in RACMO than in ERA-15 or even absent in RACMO. Comparison between RACMO output and data from Antarctic stations show that the pressure variability is correctly represented in RACMO, although the low-pressure systems are less deep in the model than the measurements indicate.

3. Meridional circulation

The classical view of the Antarctic katabatic circulation is a radially diverging boundary-layer outflow compensated for by an influx of warmer air in the middle troposphere. Figure 2a shows the RACMO 14-yr mean mass flux over the grounding line, defined as the contour line where grounded ice turns into floating
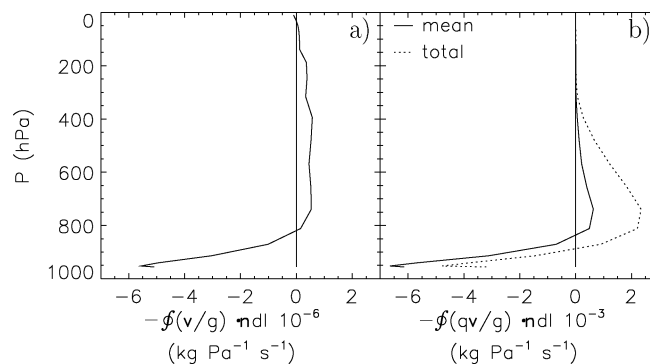
Fig. 2. Fourteen-year mean poleward mass flux (a) and moisture flux (b) across the grounding line of the Antarctic ice sheet as a function of the atmospheric pressure. Positive values indicate poleward transport. Both the moisture transport by the mean flow (solid line) and the total moisture transport (dotted line), which is the sum of the transport by the mean flow and the transport by the transient eddies, are shown.

ice (ice shelves). It is clear that, on average, mass is exported away from the Antarctic continent in a shallow layer below 800 hPa. Inflow occurs at higher atmospheric levels. This static picture is in agreement with the classical concept that off-continent flow of cold dense air regulates, by mass continuity, the poleward flow of relatively warm moist air in the higher troposphere.

The total poleward moisture flux accross the grounding line can be expressed as

$$T_q = -\oint \frac{\overline{q\boldsymbol{u}}}{g} \cdot \boldsymbol{n}\,\mathrm{d}l = T_{q,\mathrm{mean}} + T_{q,\mathrm{eddy}}$$

$$= -\oint \frac{\overline{q}\,\overline{\boldsymbol{u}}}{g} \cdot \boldsymbol{n}\,\mathrm{d}l - \oint \frac{\overline{q'\boldsymbol{u}'}}{g} \cdot \boldsymbol{n}\,\mathrm{d}l \qquad (1)$$

where q is the specific humidity, $\boldsymbol{u}$ is the horizontal wind vector, g is the acceleration due to gravity and $\boldsymbol{n}$ the unit vector directed outward, normal to grounding line. The first term on the right-hand side of eq. (1) ($T_{q,\mathrm{mean}}$) represents the contribution made by the mean flow, and the second term ($T_{q,\mathrm{eddy}}$) represents the contribution made by the eddy flux of water vapour (Schwerdtfeger, 1984). The bars indicate time averaging and the prime stands for departure from the temporal mean value.

We calculated the terms in eq. (1) by inserting modelled values of q and $\boldsymbol{u}$, available every 6 h. $T_{q,\mathrm{mean}}$ is calculated on basis of 14-yr mean values for q and $\boldsymbol{u}$. It is dominated by the katabatic winds in the boundary layer and directed toward the north, removing 51 mm water equivalents yr^{-1} (mm w.e. yr^{-1}) of moisture from the grounded ice (Fig. 2b). $T_{q,\mathrm{eddy}}$ is calculated on basis of the departure of q and $\boldsymbol{u}$ from the 14-yr mean. The eddy transport (180 mm w.e. yr^{-1}), which is not shown separately, is directed toward the pole at all levels and more than compensates for the removal by the mean flow. The largest part (83%) is transported by eddies on time scales shorter than one month. The remaining part (17%) is transported by fluctuations on time scales longer than one month. When using monthly mean values instead of 14-yr mean values to calculate $T_{q,\mathrm{mean}}$, the shape of the curve in Fig. 2b is unaffected, but the curve is shifted toward the right. The mean circulation, including fluctiations on time scales longer than one month, removes 21 mm w.e. yr^{-1} of moisture from the grounded ice. Note that Genthon and Krinner (1998) found that in ERA-15, the mean circulation transports about 10% of the total transport poleward across the 70°S latitude band.

The total poleward resolved-scale atmospheric moisture transport is 129 mm w.e. yr^{-1}. Below 875 hPa, total moisture transport is directed toward the Southern Ocean and above this level transport is directed toward Antarctica, with a maximum at 800 hPa. On average, about 20% of the inflow in the middle and higher troposphere is transported away from the continent in the lower atmosphere. In summary, the modelled mean meridional circulation at the grounding line clearly shows the characteristics of a katabatic-maintained circulation. However, it is not the mean flow, but the transient eddies that determine the moisture transport toward the grounded ice sheet.

4. Poleward atmospheric moisture transport and the surface mass balance

Since snowdrift and melt are neglected in the model, the surface mass balance is identical to the precipitation minus the sublimation. The budget equation expressing the mean surface mass balance over the grounded ice $\langle \overline{B} \rangle$ as a function of transport and storage terms is given by Peixoto and Oort (1983):

$$\langle \overline{B} \rangle = \langle \overline{P-E} \rangle = -\langle \boldsymbol{\nabla} \cdot \overline{\boldsymbol{Q}} \rangle - \frac{1}{\rho_{\mathrm{L}}} \left\langle \frac{\partial \overline{W}}{\partial t} \right\rangle, \qquad (2)$$

where the brackets indicate averaging in space, P is the precipitation, E is the sublimation, ρ_{L} is the density of water, W is the amount of water vapour contained in a unit area atmospheric column of air (kg m^{-2}) and $\boldsymbol{Q}$ is the vertically integrated horizontal moisture-flux vector, defined as

$$\boldsymbol{Q} = \frac{1}{\rho_{\mathrm{L}}} \int_0^{p_{\mathrm{s}}} \frac{q\boldsymbol{u}}{g}\,\mathrm{d}p, \qquad (3)$$

where p is the pressure. We use this definition in order to express $-\langle \boldsymbol{\nabla} \cdot \boldsymbol{Q} \rangle$ in the same units as $\langle \overline{B} \rangle$, namely water equivalents. For annual averages the second term on the right-hand side of eq. (2) is negligible (Peixoto and Oort, 1983). The atmospheric moisture transport across the grounding line of the Antarctic ice sheet can therefore be estimated from vertical profiles of q and $\boldsymbol{u}$ with the use of the Gauss theorem:

$$-\langle \boldsymbol{\nabla} \cdot \boldsymbol{Q} \rangle = -\frac{1}{A}\oint \boldsymbol{Q} \cdot \boldsymbol{n}\,\mathrm{d}l = \frac{1}{A\rho_{\mathrm{L}}}\int_0^{p_{\mathrm{s}}} T_q\,\mathrm{d}p, \quad (4)$$

where A is the surface area of the grounded ice and $\boldsymbol{n}$ the unit vector directed outward, normal to grounding line.
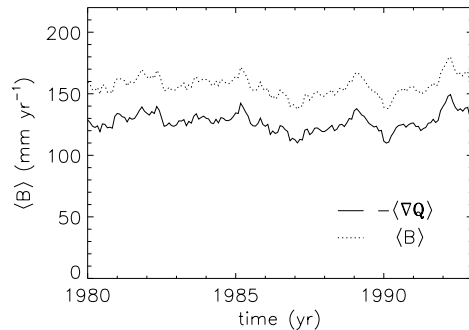
Fig. 3. Twelve-month centred running mean resolved-scale poleward atmospheric moisture transport across the grounding line (solid line) and surface mass balance of the grounded Antarctic ice sheet (dotted line).

Model output for q and $\boldsymbol{u}$, available every 6 h, is used to calculated the resolved-scale atmospheric moisture transport, which we will from now refer to as $-\langle \boldsymbol{\nabla} \cdot \boldsymbol{Q} \rangle$. Figure 3 shows the twelve-month centred running mean of $\langle B \rangle$ and $-\langle \boldsymbol{\nabla} \cdot \boldsymbol{Q} \rangle$. On average, resolved-scale flow is responsible for 81% of the moisture transport to the Antarctic grounded ice sheet. The difference between $-\langle \boldsymbol{\nabla} \cdot \boldsymbol{Q} \rangle$ and $\langle B \rangle$ is caused by (i) the horizontal diffusion of moisture in the model (this is not included in $-\langle \boldsymbol{\nabla} \cdot \boldsymbol{Q} \rangle$) and (ii) moisture transport by eddies on time-scales that are not taken into account in calculating $-\langle \boldsymbol{\nabla} \cdot \boldsymbol{Q} \rangle$, because q and $\boldsymbol{u}$ are archived at a temporal resolution of 6 h. Note that in a coarser grid GCM the difference between $-\langle \boldsymbol{\nabla} \cdot \boldsymbol{Q} \rangle$ and $\langle B \rangle$ can be much larger; Connolley and King (1996) found that only 30% of the net accumulation in the Antarctic sector between 2.4°W and 110.5°E is carried by resolved-scale transport in the UKMO GCM at a grid spacing of 270 km.

Despite the difference between $-\langle \boldsymbol{\nabla} \cdot \boldsymbol{Q} \rangle$ and $\langle B \rangle$, the temporal variability is similar. The standard deviation of annual mean values is 6–7% of the 14-yr mean value. The correlation between monthly mean values of $-\langle \boldsymbol{\nabla} \cdot \boldsymbol{Q} \rangle$ and $\langle B \rangle$ (with the annual cycle removed) is very large (0.98). Apparently, there is only small temporal variability in the effect of horizontal diffusion and eddies with short time-scales.

Genthon and Krinner (1998) studied the moisture transport in the area south of 70°S using ERA-15. The RACMO value for B south of 70°S is 20% larger than their value, which might be related to excessive sublimation/evaporation over the ice shelves which are treated as sea-ice in ERA-15. The year-to-year

variability that we found is similar to the results of Genthon and Krinner (1998). The RACMO 14-yr mean surface mass balance over the grounded ice is 156 mm w.e. yr^{-1}. This estimate is at the upper end of the most recent estimates for net accumulation [$(1528–1924) \times 10^{12}$ kg yr^{-1} (Church et al., 2001), which corresponds to 124–156 mm w.e. yr^{-1}].

Most studies on the temporal variability of moisture transport using ECMWF (re-)analyses do not focus on the Antarctic grounded ice sheet but on the Antarctic ice sheet including the ice shelves, the West Antarctic sector or the area south of 70°S. Therefore we summarise the result of a study by Van Lipzig et al. (2002), who compared RACMO and ERA-15 time series of $-\langle \boldsymbol{\nabla} \cdot \boldsymbol{Q} \rangle$ and $\langle B \rangle$ averaged over the grounded ice sheet. For both RACMO and ERA-15, the standard deviation of annual mean values is 6–7% of the 14-yr mean value, which is about half of the value found by Cullather et al. (1996) for operational analyses. The larger value for the operational analyses might be caused by the evolution of the meteorological model and assimilation techniques. The correlation between RACMO and ERA-15 montly mean values of $-\langle \boldsymbol{\nabla} \cdot \boldsymbol{Q} \rangle$ with the annual cycle removed is 0.75, which is significant at the 99% confidence level (autocorrelation effects are taken into account), indicating that the ERA-15 forcing fields determine some part of the variability of the moisture convergence in RACMO. We conclude that both $-\langle \boldsymbol{\nabla} \cdot \boldsymbol{Q} \rangle$ and $\langle B \rangle$ can be used to study the relationship between poleward atmospheric moisture transport and processes in the atmospheric boundary layer.

5. Temporal variability

We investigate what determines year-to-year variations in the surface mass balance and resolved-scale poleward atmospheric moisture transport. Were the katabatic outflow the driving force for poleward moisture advection, the outflow of moisture in the boundary layer would be positively correlated with $\langle B \rangle$, and consequently T_q in the boundary layer would be negatively correlated with $\langle B \rangle$. This is not the case. On the contrary, the correlation coefficient between T_q in the boundary-layer and $\langle B \rangle$ is positive (Fig. 4). The correlation coefficient is highest at 800 hPa, where T_q is large. Negative correlation coefficients are found in the stratosphere, but since the stratosphere is very dry, this is unimportant for surface mass balance variations. We speculate that this negative correlation stems from
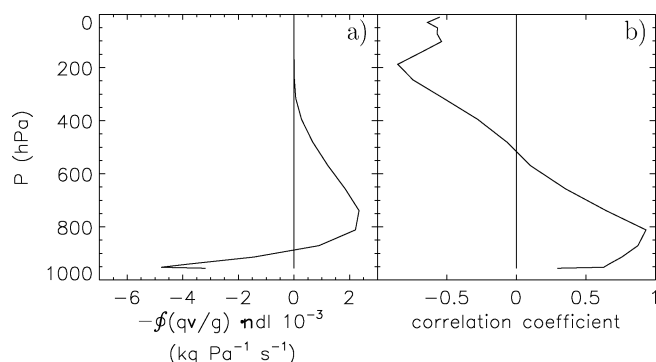
Fig. 4. Fourteen-year mean total poleward moisture flux across the grounding line of the Antarctic ice sheet (a) and correlation between annual mean values of the poleward moisture flux across the grounding line and $\langle B \rangle$ (b) as a function of the atmospheric pressure.

an intense zonal stratospheric circulation during wet years.

Annual values of $\langle B \rangle$ positively correlate with poleward mass flow from the near-surface atmospheric level to the 750 hPa level and anti-correlate with mass flow above 750 hPa (not shown). The correlation is significant at the 99% confidence level below 850 hPa. This indicates that during a year with large near-surface mass outflow and large mass convergence at higher atmospheric levels the total moisture transport toward the continent is small, supporting the idea that the moisture flux is not driven by the katabatic flow.

There is a positive correlation, significant at the 99% confidence level ($r = 0.78$), between annual values of $\langle B \rangle$ and the vertically integrated $T_{q,\text{mean}}$; during wet years, the outflow by the mean circulation is small. The correlation between $\langle B \rangle$ and $T_{q,\text{eddy}}$ is positive and significant at the 99% confidence level at pressure levels around 800 hPa, where T_q is largest. However, the positive correlation between $\langle B \rangle$ and the vertically integrated $T_{q,\text{eddy}}$ ($r = 0.44$) is not significant at the 95% confidence level.

Table 1 shows the correlation between the annual mean surface mass balance and annual mean values of some relevant meteorological variables. One would expect that wet years are also warm years, since the mean moisture content in a warm atmosphere is generally larger than in a cold atmosphere. However, flow dynamics complicates the picture, resulting in an insignificant correlation between $\langle B \rangle$ and temperature and humidity averaged over the grounded ice sheet (surface temperature, 7-m temperature, 7-m specific humidity and vertically integrated specific humidity). Also, the annual variations in source and sink terms for

Table 1. *Correlation coefficient (r) between the annual mean surface mass balance $\langle B \rangle$, averaged over the grounded ice, and either: annual mean surface temperature, 7-m temperature, 7-m specific humidity, vertically integrated specific humidity, (all averaged over the grounded ice), advection from outside the model domain, evaporation from the sea surface, precipitation on sea and meridional component of the 7-m wind speed at the grounding line*

Surface temperature	−0.11
7-m Temperature	−0.10
7-m Specific humidity	−0.01
Vertically integrated specific humidity	−0.10
Advection from outside the model domain	0.25
Evaporation from the sea surface	0.27
Precipitation on sea	0.02
7-m Meridional wind speed at the grounding line	−0.90[a]

[a]Correlation is significant at the 1% level.

moisture available for transport toward the ice sheet, namely advection from outside the model domain, evaporation from the sea surface and precipitation on sea, are not significantly correlated with annual variations in $\langle B \rangle$. Table 1 shows that the year-to-year variations in $\langle B \rangle$ are driven by the dynamics of the flow inside the model domain, as indicated by the anti-correlation (significant at the 99% confidence level) between $\langle B \rangle$ and the meridional component of the 7-m wind speed at the grounding line (defined northward as positive). The wind speed at the grounding line is calculated as the average of 489 grounded grid points which have a nearest-neighbour outside of the grounding line. On average, the meridional component of the

7-m wind speed at the grounding line is directed from land toward sea due to the katabatic forcing. We propose that during years that are more synoptically active, the katabatic wind is more frequently interrupted by events during which moist air is transported from sea to land at low atmospheric levels. This results in a relatively low annual mean meridional wind speed.

To further investigate the relationship between the dynamics of the flow in the boundary layer and annual variations in $\langle B \rangle$, we present 14-yr mean vertical profiles of the zonal wind component (u), meridional wind component (v), wind speed ($\sqrt{u^2 + v^2}$) and directional constancy (dc) at the grounding line together with the correlation between annual mean values of $\langle B \rangle$ and annual mean values of u, v, $\sqrt{u^2 + v^2}$ and dc (Fig. 5). The directional constancy (dc) is defined as

$$dc = \frac{\sqrt{\overline{u}^2 + \overline{v}^2}}{\overline{\sqrt{u^2 + v^2}}}. \tag{5}$$

Significant negative correlations at the 95% confidence level between $\langle B \rangle$ and v at the grounding line are found at the lowest five model levels up to a height of about 1 km. In addition, u is significantly positively correlated at the 99% confidence level with $\langle B \rangle$. Below about 3 km height, easterly winds prevail at the grounding line (u is negative). During wet years, the low-level zonal winds are weaker than during dry years, which is consistent with lower values for the

katabatic outflow during wet years. Higher in the troposhere (roughly above 3 km), zonal westerly winds prevail at the grounding line. During wet years, these winds are stronger than during dry years. At all tropospheric levels, the zonal westerly component of the winds at the grounding line is larger during wet years. These conditions occur when the polar vortex is strong (Van den Broeke and van Lipzig, 2002).

Correlation between $\langle B \rangle$ and wind speed reflects the direction of the wind with respect to upper-air westerlies; the correlation is significant above 2 km height (about 750 hPa), where the wind is predominantly zonal. The directional constancy in the boundary layer is low during years when the katabatic winds are frequently interrupted by passing synoptic systems. During years with a low value for the dc in the boundary layer, the moisture advection toward the ice sheet is large (hence a significant anti-correlation in Fig. 5). At higher atmospheric levels, it appears that $\langle B \rangle$ and dc are positively correlated, reflecting persistent zonal westerly winds during wet years.

Since the dynamics of the flow within the model domain influences both the year-to-year variability of the near-surface winds and the year-to-year variability of $\langle B \rangle$, we study the flow at 700 hPa. Figure 6 shows the mean geopotential at 700 hPa for the wettest and the driest years. The circumpolar trough is deep during the wet years. The circumpolar trough reflects the presence of individual low-pressure systems, which
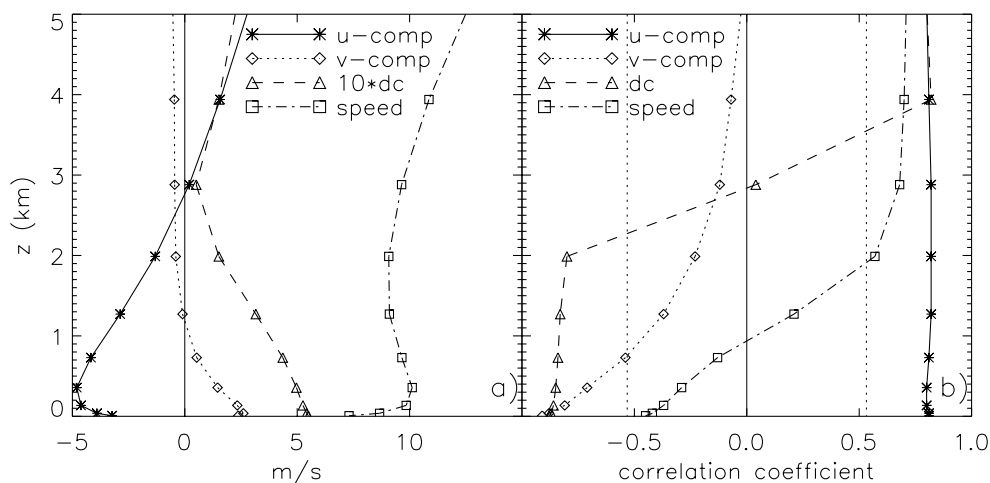
Fig. 5. Height dependency of the 14-yr mean zonal component of the wind (u; solid line), meridional component of the wind (v; dotted line), directional constancy (dc; dashed line), and wind speed ($\sqrt{u^2 + v^2}$; dotted-dashed line) averaged over the grounding line (a) and height dependency of the correlation coefficient between the annual mean $\langle B \rangle$ and the annual mean u, v, dc and $\sqrt{u^2 + v^2}$ averaged over the grounding line (b).
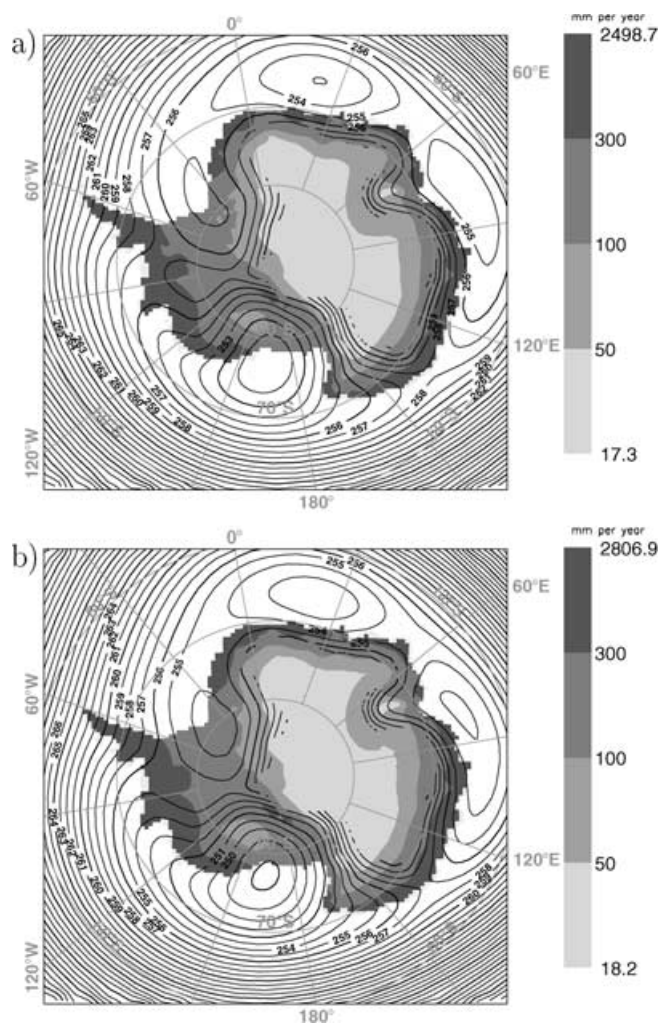
Fig. 6. Geopotential height of the 700 hPa level (contour lines; dam) and precipitation (shading; mm w.e. yr^{-1}) for the years with the lowest surface mass balance (a) and the years with the highest surface mass balance (b). The years with the lowest surface mass balance are 1980, 1983, 1986, 1987, 1988, 1990 and 1991. The years with the highest surface mass balance are 1981, 1982, 1984, 1985, 1989, 1992 and 1993.

are either more frequent or deeper during wet years. In the area north of the circumpolar trough, zonal winds are stronger during wet years.

The difference in the geopotential height at 700 hPa between the dry and the wet years is shown in Fig. 7. The meridional gradient in geopotential height is larger during wet than during dry years, indicating anomalously strong westerly geostrophic flow during wet years. However, the pattern is not zonally symmetric. Northerly flow is enhanced during wet years in the

Bellingshausen Sea and Weddell Sea coastal regions and in the western part of Wilkes Land, resulting in high precipitation in these regions. There are also regions where there is enhanced southerly flow and less precipitation (east of the Ross Ice Shelf and west of the Amery Ice Shelf). Changes in the precipitation pattern are clearly related to changes in the large-scale dynamics. The difference in surface pressure and in geopotential at 500 hPa are qualitatively similar to Fig. 7 and therefore not shown.
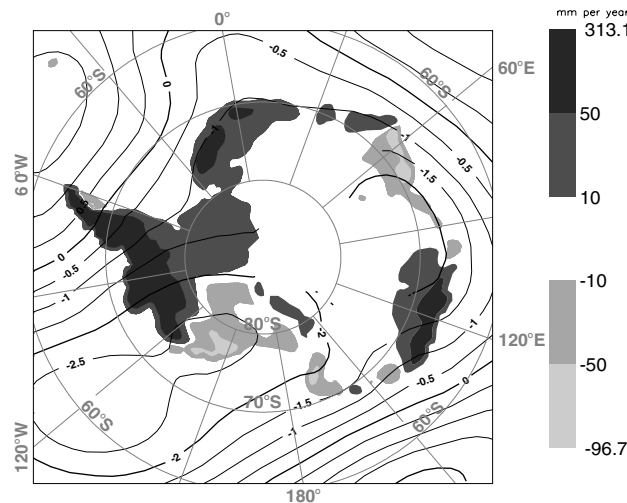
Fig. 7. Difference in geopotential height of the 700 hPa level (contour lines; dam) and precipitation (shading; mm w.e. yr^{-1}) between the years with the highest surface mass balance and the years with the lowest surface mass balance.

6. Spatial variability

The pattern of inflow and outflow of moisture is not axi-symmetric around the continent (Fig. 8). There are three regions where large inflow occurs between the 600 and 900 hPa pressure levels, namely Marie
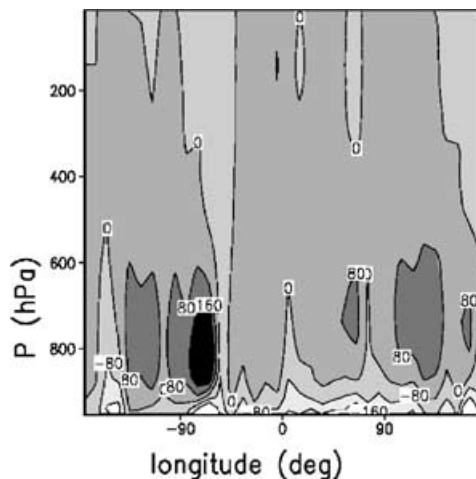
Fig. 8. Poleward atmospheric moisture flux in a longitude band of 10° (in kg Pa^{-1} s^{-1}) as a function of longitude and pressure. Positive values indicate poleward transport, dark shades indicate large poleward transport and light shades indicate northward transport.

Byrd Land (around 124°W), the western border of the Antarctic Peninsula (around 72°W) and the western part of Wilkes Land (around 124°E). At the eastern border of the Antarctic Peninsula there is outflow at all levels, since the Antarctic Peninsula is located perpendicular to the circumpolar westerly circulation, and generally the wind is directed from land toward sea. The largest outflow in the lower atmosphere occurs at the Ross Ice Shelf, the Filchner–Ronne Ice Shelf and the Amery Ice Shelf. The pattern of inflow and outflow is closely related to the geostrophic wind at 700 hPa (Fig. 6); near the ice shelves the geostrophic wind at 700 hPa is directed toward the sea.

To study the importance of different regions on the annual variations in $\langle B \rangle$, the correlation coefficient between the annual mean vertically integrated poleward atmospheric moisture transport within a longitude band of 10° and $\langle B \rangle$ was calculated. Figure 9 shows the correlation coefficient together with the vertically integrated poleward atmospheric moisture transport within a longitude band. The regions with the largest moisture inflow are again Wilkes Land, the Antarctic Peninsula, Ellsworth Land and Marie Byrd Land. The poleward atmospheric moisture transport in these regions are significantly positively correlated at the 95% confidence level with $\langle B \rangle$; variations in moisture advection in these regions are important for variations in the mean surface mass balance over the entire ice sheet. There are also regions which show an
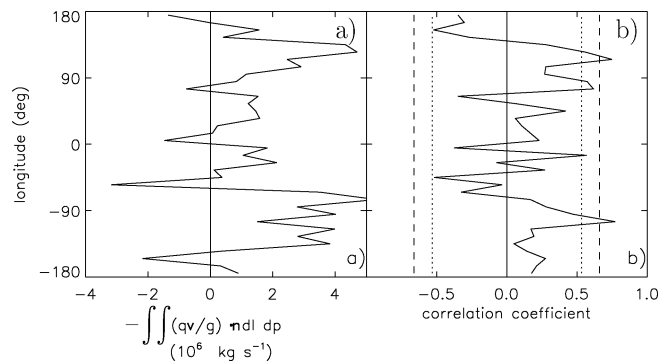
Fig. 9. Poleward atmospheric moisture transport in a longitude band of $10°$ (in 10^6 kg s^{-1}) as a function of longitude (a) and correlation between mean annual values of the surface mass balance over the grounded ice and the poleward atmospheric moisture transport in a longitude band of $10°$ (b). The dashed (dotted) lines at $r = \pm 0.66$ ($r = \pm 0.53$) indicate significant correlation at the 99% (95%) confidence level.

anti-correlation (ice shelves), but only in two of the $10°$ latitude bands in the region of the Filchner–Ronne ice shelf and the western side of the Ross Ice Shelf is this anti-correlation just statistically significant at the 95% confidence level.

7. Moisture advection during a winter month in Wilkes Land

To study time variations in poleward atmospheric moisture transport in a small region, we have selected a sector in Wilkes Land (110–130° E) where the poleward moisture transport is large. We study one winter month, July 1980. Moisture transport is clearly episodic (Fig. 10); two major events occur around 11 and 16 July. At the end of the month, several smaller events occur. From 17 to 20 July, moisture is transported away from the continent in the Wilkes Land sector.

To study the relationship between boundary-layer flow and atmospheric moisture transport, we average the meteorological variables over two bulk layers. In the lower layer, extending from the surface to 500 m, the mean meridional wind component is directed toward the sea (Fig. 11). In the upper layer, extending from 500 m to 7 km, inflow of moisture takes place, except from 17 to 20 July, when flow at all levels is toward the sea (Fig. 12). From 17 to 20 July the specific humidity in both layers drops significantly to values well below 1 g kg^{-1}. This decrease in specific humidity, caused by the change in wind direction, reduces the amount of moisture that is transported in the atmosphere during this event.

During the events of large poleward advection of moisture at 11 and 16 July, the northerly component of the wind in the upper layer is at a local maximum. The geopotential height of the 700 hPa level and the 6 h accumulated precipitation at 12 UTC 11 July are
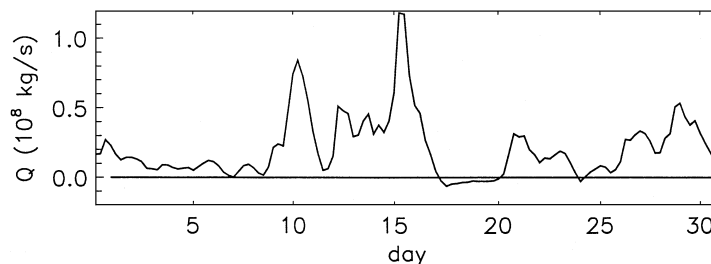
Fig. 10. Poleward atmospheric moisture transport across the grounding line in the longitude band 110–130° E (Wilkes Land) during July 1980 as a function of day of the month. Note that the time interval on which model output is available is 6 h.
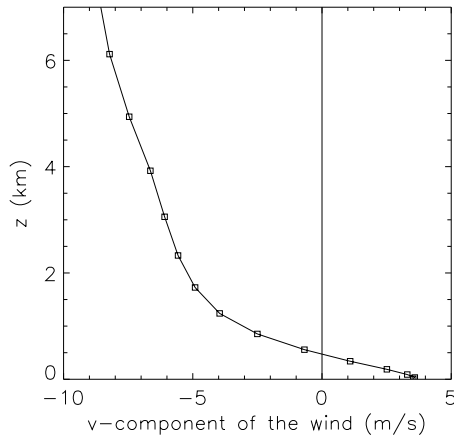
Fig. 11. Monthly mean meridional component of the wind at the grounding line in the longitude band 110–130°E (Wilkes Land) for July 1980 as a function of height. Model output is averaged over the grid boxes, representing grounded ice, in the longitude band 110–130°E (Wilkes Land) which have a nearest neighbour outside the grounding line.

shown in Fig. 13. The strong northerly winds in the sector 110–130°E are caused by a low pressure system at 80°E. This, together with the increase in specific humidity at the upper level, results in large poleward advection of moisture and high precipitation rates in the Wilkes Land sector.

Figure 12 strongly suggests that the boundary layer and middle/higher troposphere reacts passively to the occurrence of the synoptic systems. Mostly, the meridional component of the wind in the boundary layer follows that of the higher troposphere. This indicates that the katabatic force is not the main driving force for moisture exchange. Note that there are several days when northerly wind occurs below 500 m. Also the specific humidity in the boundary layer follows the higher troposphere, with a time lag. Both northerly and southerly moisture advection occurs in the lower layer, but it is much smaller than the moisture advection above 500 m. We conclude that variations of the moisture advection in the boundary layer in Wilkes Land during July 1980 are insignificant for moisture exchange between the ice sheet and the surrounding oceans.

8. Conclusions

In this paper we have used a regional atmospheric model, forced at the lateral boundaries by ERA-15 data, to study the relationship between boundary-layer
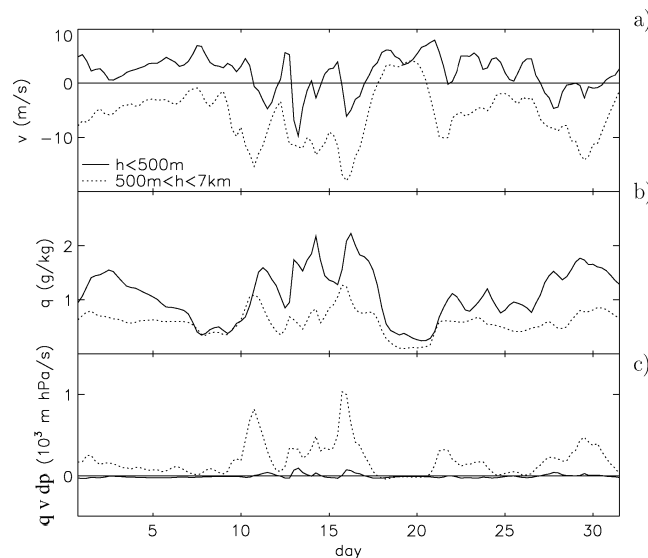
Fig. 12. Time series of the meridional component of the wind v (a), specific humidity q (b) and poleward moisture transport (c) in the layer from the surface to 500 m height (solid line) and in the layer from 500 m to 7 km height (dotted line). Values of v and q are averaged over the grid boxes, representing grounded ice, in the longitude band 110–130°E (Wilkes Land) which have a nearest neighbour outside the grounding line. $qvdp$ is the advection of moisture over the grounding line in the same longitude band. The values are plotted for July 1980 as a function of the day.
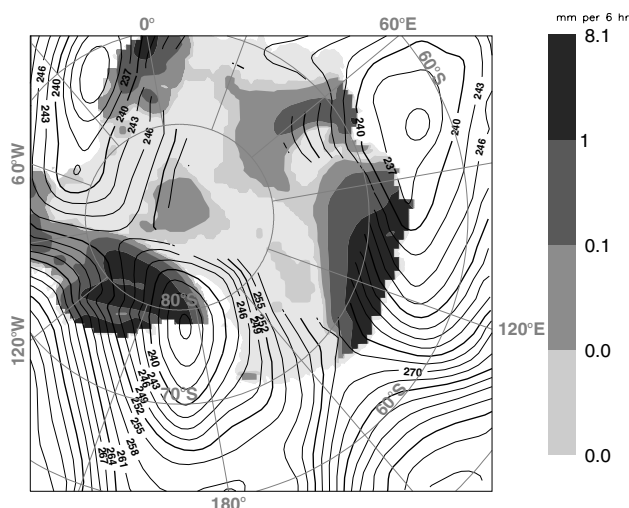
Fig. 13. Geopotential height of the 700 hPa level (contour lines; dam) and precipitation over the previous 6 h (shading; mm w.e. per 6 h) for 12 UTC 11 July 1980.

processes and poleward atmospheric moisture transport toward the grounded Antarctic ice. The net poleward atmospheric moisture transport $(-\langle \nabla \cdot \boldsymbol{Q} \rangle)$ in RACMO is determined by the transport of water vapour and does not include blowing snow. Our results show the importance of synoptic-scale dynamics of the flow; in the 14-yr integration, the flow within the model domain controls variations in $-\langle \nabla \cdot \boldsymbol{Q} \rangle$.

The classical picture of a katabatic circulation shows an outflow of cold air in the lower atmosphere, inducing, by mass continuity, an inflow of relatively warm moist air at higher levels. We studied whether moisture inflow at higher levels responds passively to the katabatic outflow. Were this the case, $-\langle \nabla \cdot \boldsymbol{Q} \rangle$ would be largest when the katabatic outflow is largest. However, our results show that the opposite is true; the boundary layer responds passively to the synoptic systems rather than being the driving force of meridional moisture exchange. During years with weak mean katabatic winds, $-\langle \nabla \cdot \boldsymbol{Q} \rangle$ is large. These wet years generally have a deep circumpolar trough and a low value in the boundary layer both for the directional constancy and for the mean southerly and mean easterly components of the wind. All these phenomena indicate that during wet years the prevailing katabatic winds are frequently interrupted by the influence of low-pressure systems. In the higher troposphere, stronger than average westerly winds with a high value for the directional constancy are present during wet years. These conditions prevail

when the polar vortex is strong (Van den Broeke and van Lipzig, 2002) resulting in weakening of the downslope, easterly near-surface winds, by the large-scale pressure gradient force.

Without considering changes in flow dynamics, wet years are likely to correspond to warm and humid atmospheric conditions. However, we did not find a significant correlation between surface mass balance and temperature or humidity for annual mean values. The results confirm that the large-scale dynamics of the flow are dominant in forcing annual variations in the poleward moisture transport.

9. Acknowledgements

REFERENCES

British Antarctic. Survey, Scott Polar Research Institute and World Conservation Monitoring Centre 1993. *Antarctic Digital Database User's Guide and Reference Manual.* Scientific Committee on Antarctic Research, Cambridge, 167 pp.

Bromwich, D. H., Robasky, F. M. and Cullather, R. I. 1995. The atmospheric hydrologic cycle over the Southern Ocean and Antarctica from operational numerical analyses. *Mon. Wea. Rev.* **123**, 3518–3538.

Bromwich, D. H., Rogers, A. N., Kållberg, P., Cullather, R. I., White, J. W. C. and Kreutz, K. J. 2000. ECMWF analyses and reanalyses depiction of ENSO signal in Antarctic Precipitation *J. Clim.* **13**, 1406–1420.

Budd, W. F., Reid, P. A. and Minty, L. J. 1995. Antarctic moisture flux and net accumulation from global atmospheric analyses. *Ann. Glaciol.* **21**, 149–156.

Christensen, J. H. and van Meijgaard, E. 1992. *On the construction of a Regional Atmospheric Climate Model.* Technical Report No. 147, Royal Netherlands Meteorological Institute, de Bilt, 22 pp.

Christensen, J. H., Christensen, O. B., Lopez, P., van Meijgaard, E. and Botzet, M. 1996. *The* HIRAM4 *Regional Atmospheric Climate Model.* DMI Scientific Report 96-4, Copenhagen, 51 pp.

Church, J. A., Gregory, J. M., Huybrechts, P., Kuhn, M., Lambeck, K., Nhuan, M. T., Qin, D. and Woodworth, P. L. 2001. Changes in sea level. In: *Climate Change 2001: The Scientific Basis. Contribution of Working Group I to the Third Assessment Report of the Intergovernmental Panel on Climate Change* (eds. J. T., Houghton, Y. Ding, D. J. Griggs, M. Noguer, P. J. van der Linden and D. Xiaosu) Cambridge University Press, 944 pp.

Connolley, W. and Cattle, H. 1994. The Antarctic climate of the UKMO unified model. *Ant. Sci.* **6**, 115–122.

Connolley, W. M. and King, J. C. 1993. Atmospheric water-vapour transport to Antarctica inferred from radiosonde data. *Q.J.R. Meteorol. Soc.* **119**, 325–342.

Connolley, W. M. and King, J. C. 1996. A modeling and observational study of the East Antarctic surface mass balance. *J. Geophys. Res.* **101**, D1, 1335–1343.

Connolley, W. M., and Harangozo, S. A. 2001. A comparison of five numerical weather prediction analysis climatologies in Southern high latitudes. *J. Clim.* **14**, 30–44.

Cullather, R. I., Bromwich, D. H. and Grumbine, R. W. 1997a. Validation of operational numerical analyses in Antarctic latitudes. *J. Geophys. Res.* **102**, D12, 13761–13784.

Cullather, R. I., Bromwich, D. H. and Van Woert, M. L. 1997b. Spatial and temporal variability of Antarctic precipitation from atmospheric methods. *J. Clim.* **11**, 334–367.

Cullather, R. I., Bromwich, D. H. and Van Woert, M. L. 1996. Interannual variations in Antarctic precipitation related to El Niño-Southern Oscillation. *J. Geophys. Res.* **101**, D14, 19109–19118.

Dalu, G. A., Baldi, M., Moran, M. D., Nardone, C. and Sbano, L. 1993. Climate atmospheric outflow at the rim of the Antarctic continent. *J. Geophys. Res.* **98**, D7, 12955–12960.

Dansgaard, W. 1964. Stable isotopes in precipitation. *Tellus* **16**, 436–468.

Davies, H. C. 1976. A lateral boundary formulation for multi-level prediction models. *Q. J. R. Meteorol. Soc.* **102**, 405–418.

Dethloff K., Abegg, C., Rinke, A., Hebestadt, I. and Romanov, V. F. 2001. Sensitivity of Arctic climate simulations to different boundary-layer parameterizations in a regional climate model. *Tellus* **53A**, 1–26.

Gallée, H. 1996. Mesoscale atmospheric circulations over the Southwestern Ross Sea sector, Antarctica. *J. Appl. Meteorol.* **35**, 1129–1141.

Gallée, H., Guyomarc'h, G. and Brun, E. 2001. Impact of snow drift on the Antarctic ice sheet surface mass balance: possible sensitivity to snow-surface properties. *Boundary-Layer Meteorol.* **99**, 1–19.

Genthon, C. and Krinner, G. 1998. Convergence and disposal of energy and moisture on the Antarctic polar cap from ECMWF reanalyses and forecasts. *J. Clim.* **11**, 1703–1716.

Gibson, R., Kållberg, P., Uppala, S., Hernandez, A., Nomura, A. and Serrano, E. 1997. ERA *Description*. Re-Analysis Project Report Series No. 1, European Centre for Medium-Range Weather Forecasts (ECMWF), Reading, UK, 72 pp.

Giovinetto, M. B., Bromwich, D. H. and Wendler, G. 1992. Atmospheric net transport of water vapor and latent heat across 70°S. *J. Geophys. Res.* **97**, D1, 917–930.

Gustafsson, N. 1993. HIRLAM 2 *Final Report*. HIRLAM Tech. Report No. 9, SMHI, Norrköping, Sweden.

Heinemann, G. 1997. Idealized simulations of the Antarctic katabatic wind system with a three-dimensional mesoscale model. *J. Geophys. Res.* **102**, D12, 13825–13834.

James, I. N. 1989. The Antarctic drainage flow: implications for hemispheric flow on the southern hemispere. *Antarctic Sci.* **I**, 279–290.

Johnsen, S. W., Dansgaard, W., Clausen, H. B. and Langway, C. C. Jr. 1972. Oxygen isotope profiles through the Antarctic and Greenland ice sheets. *Nature* **235**, 429–434.

King, J. C., Connolley, W. M. and Derbyshire, S. H. 2001. Sensitivity of modelled Antarctic climate to surface and boundary layer flux parameterizations. *Q.J.R. Meteorol. Soc.* **127**, 779–794.

Krinner, G., Genthon, C. and Jouzel, J. 1997. GCM analysis of local influences on ice core signals. *Geophys. Res. Lett.* **24**, 2825–2828.

Lenderink, G. and van Meijgaard, E. 2001. Impacts of cloud and turbulence schemes on integrated water vapor: comparison between model predictions and GPS measurements. *Meteorol. Atmos. Phys.* **77**, 131–144.

Louis, J. F. 1979. A parametric model of vertical eddy fluxes in the atmosphere. *Boundary Layer Meteorol.* **17**, 187–202.

Marshall, G. J. 2000. An examination of the precipitation regime at Thurston Island, Antarctica, from ECMWF reanalysis data. *Int. J. Climatol.* **20**, 255–277.

Murphy, B. F. and Simmonds, I. 1993. An analysis of strong wind events simulated in a GCM near Casey in the Antarctic. *Mon. Wea. Rev.* **121**, 522–534.

Noone, D., Turner, J. and Mulvaney, R. 1999. Atmospheric signals and characteristics of accumulation in Dronning Maud Land, Antarctica. *J. Geophys. Res.* **104**, D16, 19191–19211.

Parish, T. R. and Bromwich, D. H. 1991. Continental-scale simulation of the Antarctic katabatic wind regime. *J. Clim.* **4**, 135–146.

Parish, T. R. and Bromwich, D. H. 1998. A case study of Antarctic katabatic wind interaction with large-scale forcing. *Mon. Wea. Rev.* **126**, 199–209.

Parish, T. R., Pettre, P. and Wendler, G. 1993. The influence of large scale forcing on the katabatic wind regime of Adelie Land, Antarctica. *Meteorol. Atmos. Phys.* **51**, 165–176.

Parish, T. R., Bromwich, D. H. and Tzeng, R.-Y. 1994. On the role of the Antarctic continent in forcing large-scale circulations in the high southern latitudes. *J. Atmos. Sci.* **51**, 3566–3579.

Peel, D. A., Mulvaney, R., Pasteur, E. C. and Chenery, C. 1996. Climate change in the Atlantic sector of Antarctic over the past 500 years from ice-cores and other evidence. In: *Climate variations and forcing mechanisms of the last 2000 years* (eds. P. D. Jones, R. S. Bradley and J. Jouzel). Springer-Verlag, Berlin, 243–262.

Peixoto, J. P. and Oort, A. H. 1983. The atmospheric branch of the hydrological cycle and climate. In: *Variations in the global water budget* (eds. A. Street-Perrott, M. Beran and R. Ratcliff). Reidel, Dordrecht, 5–65.

Reijmer, C. H. and van den Broeke, M. R. 2001. Moisture sources of precipitation in Western Dronning Maud Land, Antarctica. *Antarctic Sci.* **13**, 210–220.

Roeckner, E., Arpe, K., Bengtsson, L., Christoph, M., Claussen, M., Dümenil, L., Esch, M., Giorgetta, M., Schlese, U. and Schulzweida, U. 1996. *The atmospheric general circulation model* ECHAM-4*: Model description and simulation of present-day climate.* Max-Planck Institut für Meteorologie, Report no. 218.

Schlosser, E., van Lipzig, N. P. M. and Oerter, H. 2002. Temporal variability of accumulation at Neumayer station, Antarctica from stake array measurements and a regional atmopsheric model. *J. Glac.* **48**(160), 87–94.

Schwerdtfeger, W. 1984. Weather and climate of the Antarctic. In: *Developments in atmospheric science*, **15**, Elsevier, Amsterdam, 261 pp.

Sundqvist, H. 1978. A parameterization scheme for nonconvective condensation including prediction of cloud water content. *Quart. J. R. Meteorol. Soc.* **104**, 677–690.

Steig, E. J., Grootes, P. M. and Stuiver, M. 1994. Seasonal precipitation timing and ice core records. *Science* **266**, 1885–1886.

Turner, J., Connolley, W. M., Leonard, S., Marshall, G. J. and Vaughan, D. 1999. Spatial and temporal variability of net snow accumulation over the Antarctic from ECMWF re-analysis project data. *Int. J. Climatol.* **19**, 697–724.

Turner, J., Lachlan-Cope, T. A., Marshall, G. J., Pendlebury, S. and Adams, N. 2001. An extreme wind event at Casey station, Antarctica. *J. Geophys. Res.* **106**, D7, 7291–7311.

Tzeng, R.-Y., Bromwich, D. H. and Parish, T. R. 1993. Present-day Antarctic climatology of the NCAR community climate model version I. *J. Clim.* **6**, 205–226.

Van den Broeke, M. R., van de Wal, R. S. W. and Wild, M. 1997. Representation of Antarctic katabatic winds in a high-resolution GCM and a note on their climate sensitivity. *J. Clim.* **10**, 3111–3129.

Van den Broeke, M. R., van Lipzig, N. P. M., van Meijgaard, E. and Oerlemans, J. 2002. Momentum budget of the East-Antarctic atmospheric boundary layer: results of a regional climate model. *J. Atmos. Sci.* (in press).

Van den Broeke, M. R. and van Lipzig, N. P. M. 2002. Impact of large scale circulation variability on the East Antarctic atmospheric boundary layer. *Tellus* **54A**, this issue.

Van den Hurk, B. J. J. M., Graham, L. P. and Viterbo, P. 2002. Comparison of land surface hydrology in regional climate simulations of the Baltic Sea catchment. *J. Hydrol.* **255**, 169–193.

Van Lipzig, N. P. M. 1999. *The surface mass balance of the Antarctic ice sheet: a study with a regional atmospheric climate model.* Thesis, Utrecht University, ISBN 90-39302208-2, 154 pp.

Van Lipzig, N. P. M., van Meijgaard, E. and Oerlemans, J. 1998. Evaluation of a regional atmospheric climate model using in situ measurements from Antarctica. *Ann. Glac.* **27**, 507–514.

Van Lipzig, N. P. M., van Meijgaard, E. and Oerlemans, J. 1999. Evaluation of a regional atmospheric climate model using measurements of surface heat exchange processes from a site in Antarctica. *Mon. Wea. Rev.* **127**, 1994–2001.

Van Lipzig, N. P. M., van Meijgaard, E. and Oerlemans, J. 2002. The spatial and temporal variability of the surface mass balance in Antarctica: results from a regional climate model. *Int. J. Climatol.* **22**, 1197–1217.

Van Meijgaard, E., Andrae, U. and Rockel, B. 2001. Comparison of model predicted cloud parameters and surface radiative fluxes with observations on the 100 km scale. *Meteorol. Atmos. Phys.* **77**, 109–130.

Wendler, G., Stearns, C., Weidner, G., Dargaud, G. and Parish, T. 1997. On the extraordinary katabatic winds of Adelie Land. *J. Geophys. Res.* **102**, D4, 4463–4474.